Journal of Advanced Ceramics
2013, 2(4): 308–312
DOI: 10.1007/s40145-013-0076-7

ISSN 2226-4108
CN 10-1154/TQ

Research Article

Theoretical investigations on electrocaloric properties of (111)-oriented $PbMg_{1/3}Nb_{2/3}O_3$ single crystal

Mahmoud Aly HAMAD*

Physics Department, *Faculty of Science*, *Tanta University*, *Tanta*, *Egypt*

Received: April 07, 2013; Revised: June 20, 2013; Accepted: August 07, 2013

Abstract: The electrocaloric (EC) effect accompanied with the ferroelectric to paraelectric phase transition in (111)-oriented $PbMg_{1/3}Nb_{2/3}O_3$ (PMN) is investigated. It is shown that the largest change ΔT is 0.37 K in 3 kV/cm electric field shift near the Curie temperature of 221 K; that is, the cooling ΔT per unit field (MV/m) is 1.23×10^{-6} m·K/V. This value is significantly larger, and comparable with the value of 0.254×10^{-6} m·K/V for $PbZr_{0.95}Ti_{0.05}O_3$ thin film under larger electric field shift ΔE = 30 kV/cm. Thus, the EC effect of (111) PMN single crystal provides cooling solutions at low temperatures, and opens more opportunities for practical application in cooling systems.

Keywords: electrocaloric (EC) effect; $PbMg_{1/3}Nb_{2/3}O_3$ (PMN); model; polarization; entropy change; heat capacity change

1 Introduction

The electrocaloric (EC) effect or magnetocaloric effect provides an efficient approach to realize solid-state cooling devices instead of the existing vapor compression refrigeration [1–16]. Ferroelectric refrigeration is based on the EC effect, an entropy change of ferroelectric material during application or withdrawal of electric field.

$PbMg_{1/3}Nb_{2/3}O_3$ (PMN) ferroelectric materials with compositions near the morphotropic phase boundary are promising for high-strain actuators/transducers and prototype microelectro-mechanical systems due to their well-known ferroelectric, dielectric and piezoelectric properties [17–23]. In this paper, the dependence of polarization on variation of temperature for (111)-oriented PMN at low electric field is simulated to predict electrocaloric properties under applied electric field shift ΔE (defined as $E_2 - E_1$).

* Corresponding author.
E-mail: m_hamad76@yahoo.com

2 Theoretical considerations

According to the phenomenological model [24], the dependence of polarization on variation of temperature and Curie temperature T_C is presented by

$$P = \left(\frac{P_i - P_f}{2}\right)\{\tanh[A(T_C - T)]\} + BT + C \qquad (1)$$

where P_i is the initial value of polarization at ferroelectric–paraelectric transition and P_f is the final value of polarization at ferroelectric–paraelectric transition as shown in Fig. 1.

$$A = \frac{2\left(B - \left.\frac{dP}{dT}\right|_{T=T_C}\right)}{P_i - P_f}$$

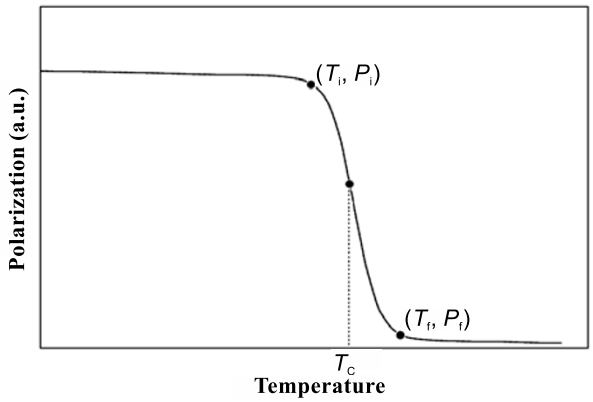

Fig. 1 Dependence of polarization as a function of temperature described by Eq. (1).

B is the polarization sensitivity $\frac{\mathrm{d}P}{\mathrm{d}T}$ at ferroelectric state before transition; $\left.\frac{\mathrm{d}P}{\mathrm{d}T}\right|_{T=T_C}$ is the polarization sensitivity $\frac{\mathrm{d}P}{\mathrm{d}T}$ at Curie temperature T_C; and $C = \frac{P_f + P_i}{2} - BT_C$.

Equation (1) is determined by the physical mechanism that the dipole-ordered state can be enhanced by decreasing temperature. At the transition temperature, the spontaneous polarization forms surface charges and stray charges accumulate on the surface of ferroelectric material. When there is non-homogeneous distribution of the spontaneous polarization, the surface charges produce an electric field, denoted as depolarization field which is in the opposite direction to the spontaneous polarization.

As a result of this phenomenological model, the electrocaloric entropy change ΔS^E caused by variation of the external electric field from E_1 to E_2 is given by

$$\Delta S^E = \left\{-A\left(\frac{P_i - P_f}{2}\right)\mathrm{sech}^2[A(T_C - T)] + B\right\}\frac{\Delta E}{\rho} \quad (2)$$

where ρ is the mass density.

A main result of Eq. (2) is that the maximum entropy change ΔS^E_{max} (where $T = T_C$) can be expressed as the following expression:

$$\Delta S^E_{max} = \left[-A\left(\frac{P_i - P_f}{2}\right) + B\right]\Delta E / \rho \quad (3)$$

According to the phenomenological model [24], the full-width at half-maximum (FWHM) δT_{FWHM} can be calculated as

$$\delta T_{FWHM} = \frac{2}{A}\cosh^{-1}\left[\sqrt{\frac{2A(P_i - P_f)}{A(P_i - P_f) + 2B}}\right] \quad (4)$$

The electrocaloric cooling efficiency is calculated by considering the magnitude of maximum electrocaloric entropy change, $-\Delta S^E_{max}$, and its FWHM (δT_{FWHM}) [25]. A product of $-\Delta S^E_{max}$ and δT_{FWHM} is called the relative cooling power (RCP) based on electrocaloric entropy change:

$$\begin{aligned}\mathrm{RCP} &= -\Delta S^E_{max}(T, \Delta E) \times \delta T_{FWHM} \\ &= \left(P_i - P_f - 2\frac{B}{A}\right)\frac{\Delta E}{\rho} \times \cosh^{-1}\left[\sqrt{\frac{2A(P_i - P_f)}{A(P_i - P_f) + 2B}}\right]\end{aligned} \quad (5)$$

The polarization-related change of heat capacity is given by

$$\Delta C_{P,E} = T\frac{\delta \Delta S^E}{\delta T} \quad (6)$$

According to this phenomenological model, the change of heat capacity is given by

$$\begin{aligned}\Delta C_{P,E} = &-2TA^2\left(\frac{P_i - P_f}{2}\right)\mathrm{sech}^2[A(T_C - T)] \\ &\times \tanh[A(T_C - T)]\Delta E/\rho\end{aligned} \quad (7)$$

The temperature change of a polar system under adiabatic electric field variation from an initial value E_1 to a final value E_2 can be written in the form:

$$\begin{aligned}\Delta T &= -\frac{T}{C_E \rho}\int_{E_1}^{E_2}\left(\frac{\partial P}{\partial T}\right)_E \mathrm{d}E \\ &= \frac{AT(P_i - P_f)}{2C_E \rho}\{\mathrm{sech}^2[A(T_C - T)] + B\}\Delta E\end{aligned} \quad (8)$$

C_E is the heat capacity per mole at constant electric field.

The refrigerant capacity (RC) is the amount of heat that can be transferred in one thermodynamic cycle [26]. Here, RC value can be obtained as [24]

$$\begin{aligned}\mathrm{RC} &= \int_{T_C - \frac{\delta T_{FWHM}}{2}}^{T_C + \frac{\delta T_{FWHM}}{2}} \Delta S^E \mathrm{d}T \\ &= \left[-(P_i - P_f)\tanh\left(A\frac{\delta T_{FWHM}}{2}\right) + B\delta T_{FWHM}\right]\frac{\Delta E}{\rho}\end{aligned} \quad (9)$$

From this phenomenological model, it can easily calculate the values of δT_{FWHM}, $|\Delta S^E|_{max}$, $|\Delta T|_{max}$, RCP, RC and ΔC_{min} due to applied electric field shift ΔE.

3 Simulation

In order to apply the phenomenological model, five parameters versus applied electric field were determined as displayed in Table 1. The heat capacity C_P is 320 J/(kg·K) and the mass density ρ is 8.3 g/cm^3 [20]. Figure 2 shows polarization versus temperature for (111) PMN under different electric fields. The symbols represent the experimental data from Ref. [27] and the dashed lines represent the modelled data. It shows a good agreement between the modelled results and experimental data. Figures 3–5 illustrate the predicted entropy changes, heat capacity changes and temperature changes versus temperature due to different electric field shifts calculated from Eqs. (2), (7) and (8), respectively.

Table 2 shows the calculated values of δT_{FWHM}, $|\Delta S^E|_{\max}$, $|\Delta T|_{\max}$, RCP, RC, $\Delta C_{\min}$ and $\Delta C_{\max}$ for (111) PMN due to applied electric field shift ΔE. It is clear that as ΔE increases, the values of $|\Delta T|_{\max}$, $|\Delta S^E|_{\max}$, RCP, RC, $-\Delta C_{\min}$ and $\Delta C_{\max}$ increase.

Under low applied electric field shift ΔE = 3 kV/cm, the peak value of ΔS of (111) PMN is 0.54 J/(kg·K). This indicates that (111) PMN is significant, and comparable with value of the best electrocaloric material ($PbZr_{0.95}Ti_{0.05}O_3$ thin film) which has peak values of $\Delta S = 0.6$ J/(kg·K) under larger electric field shift $\Delta E = 30$ kV/cm [1].

Table 1 Model parameters for (111) PMN single crystal due to applied electric field

E	T_C	P_i	P_f	B	$\left.\frac{dP}{dT}\right\|_{T=T_C}$
(kV/cm)	(K)	(C/m^2)	(C/m^2)	(C/(m^2·K))	(C/(m^2·K))
1.5	230	0.128	0.009	–0.000 10	–0.001
2.0	199	0.276	0.088	–0.000 60	–0.015
2.5	209	0.277	0.083	–0.000 55	–0.015
3.0	221	0.280	0.085	–0.000 60	–0.015

Table 2 Calculated values of electrocaloric properties of (111) PMN single crystal at different electric field shifts

ΔE	δT_{FWHM}	$\lvert\Delta S^E\rvert_{\max}$	$\lvert\Delta T\rvert_{\max}$	RCP	RC	$\Delta C_{\min}$	$\Delta C_{\max}$
(kV/cm)	(K)	(J/(kg·K))	(K)	(J/kg)	(J/kg)	(J/(kg·K))	(J/(kg·K))
1.5	127.25	0.02	0.01	2.29	1.83	–0.04	0.05
2.0	11.90	0.36	0.22	4.29	3.44	–7.65	8.29
2.5	12.20	0.45	0.29	5.50	4.41	–10.19	10.23
3.0	12.34	0.54	0.37	6.68	5.35	–12.31	13.32

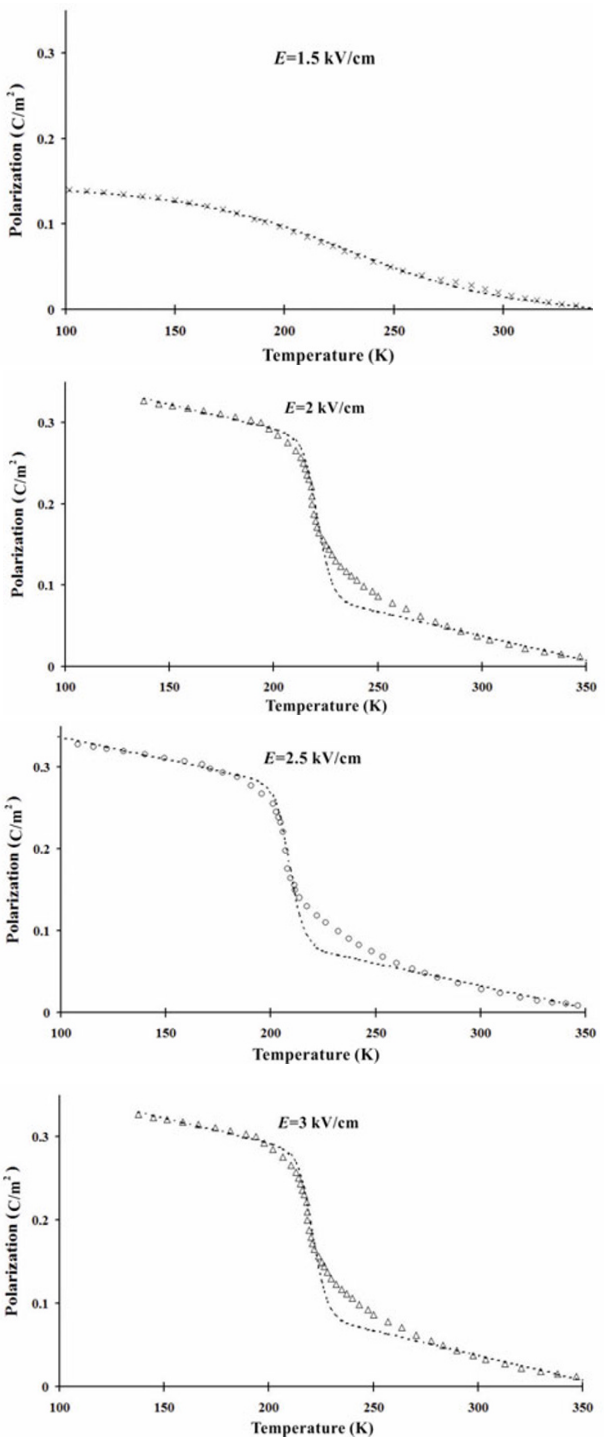

Fig. 2 Polarization variation induced by temperature change under different electric fields for (111) PMN single crystal. The dashed lines are modeled results by Eq. (1) and symbols represent experimental data from Ref. [27].

It is clear that as the temperature is far away from the Curie temperature, the entropy change with increasing temperature is not very noticeable, so the

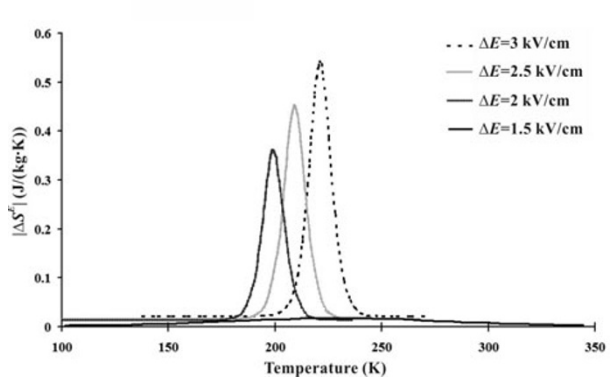

Fig. 3 Absolute values of electrocaloric entropy changes versus temperature due to applied electric field shifts for (111) PMN single crystal. They are obtained by Eq. (2) at different electric field shifts.

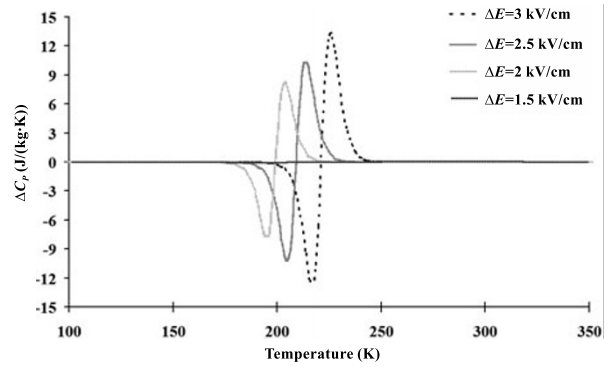

Fig. 4 Heat capacity changes for (111) PMN single crystal due to applied electric field shifts ΔE versus temperature. They are obtained by Eq. (7) at different electric field shifts.

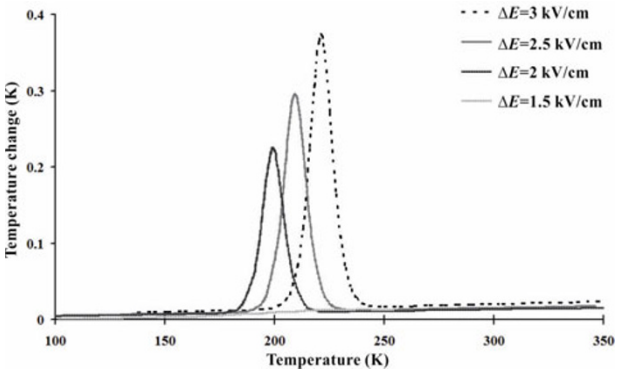

Fig. 5 Electrocaloric temperature changes ΔT due to applied electric field shifts ΔE versus temperature for (111) PMN single crystal. They are obtained by Eq. (8) at different electric field shifts.

electrocaoric temperature change ΔT is small. When the temperature rises close to T_C, the large entropy change is induced by an external strong electric field during the ferroelectric–paraelectric phase transition, so ΔT becomes large. When the temperature is above and far from T_C, due to the presence of only paraelectric phase, a small entropy change with rising temperature decreases ΔT sharply. This is why a large EC effect and the peak of ΔT occur near T_C, as shown in Fig. 5. Furthermore, the entropy change curves reveal the characteristics of the dipole reorientation by the kinks in the ΔS^E curves. The maxima observed in the ΔS^E curve are associated to a dipole reorientation that occurs continuously. Therefore, the behavior of ΔS^E suggests how to extend the range of temperatures for use in the EC effect.

In Fig. 5, the largest change ΔT is 0.37 K in 3 kV/cm electric field shift; that is, the cooling ΔT per unit field (MV/m) is 1.23×10^{-6} m·K/V. This value is significantly larger, and comparable with the value of 0.254×10^{-6} m·K/V for $PbZr_{0.95}Ti_{0.05}O_3$ thin film under larger electric field shift $\Delta E = 30$ kV/cm. The results indicate the potential of PMN single crystal to achieve an EC effect because of the large entropy change associated with the electric field-induced dipole ordering–disordering (O–D) processes at temperatures near the O–D transformations. In addition, the electrical properties of ferroelectric single crystals are dependent on many condition parameters, such as composition, preferential orientation, and so on [28].

Finally, in this phenomenological model, it can calculate the electrocaloric properties of PMN single crystal with limited processing time. Moreover, the model does not add any auxiliary computational efforts to the numerical simulation.

4 Conclusions

It is investigated that the ferroelectric–paraelectric transition of (111) PMN single crystal under low applied electric fields, and found that the large EC effect induced by the ferroelectric–paraelectric phase transition at low electric field. The calculations show that the cooling ΔT per unit field of (111) PMN single crystal in 3 kV/cm electric field shift near the Curie temperature of 221 K is larger than that of $PbZr_{0.95}Ti_{0.05}O_3$ thin film under larger electric field shift $\Delta E = 30$ kV/cm. Thus, the EC effect of (111) PMN single crystal provides cooling solutions at low temperatures. Moreover, the pyroelectric effect could

be used for example to recover useful electrical power from waste heat.

References

[1] Hamad MA. Investigations on electrocaloric properties of [111]-oriented $0.955PbZn_{1/3}Nb_{2/3}O_3$–$0.045PbTiO_3$ single crystals. *Phase Transitions* 2013, **86**: 307–314.

[2] Hamad MA. Giant electrocaloric effect of highly (100)-oriented $0.68PbMg_{1/3}Nb_{2/3}O_3$–$0.32PbTiO_3$ thin film. *Phil Mag Lett* 2013, **93**: 346–355.

[3] Hamad MA. Detecting giant electrocaloric properties of ferroelectric SbSI at room temperature. *J Adv Dielect* 2013, DOI: 10.1142/S2010135X13500082.

[4] Hamad MA. Investigations on electrocaloric properties of ferroelectric $Pb(Mg_{0.067}Nb_{0.133}Zr_{0.8})O_3$. *Appl Phys Lett* 2013, **102**: 142908.

[5] Hamad MA. Magnetocaloric effect in $La_{0.65-x}Eu_xSr_{0.35}MnO_3$. *Phase Transitions* 2012, DOI:10.1080/01411594.2013.828056.

[6] Hamad MA. Theoretical work on magnetocaloric effect in $La_{0.75}Ca_{0.25}MnO_3$. *J Adv Ceram* 2012, **1**: 290–295.

[7] Hamad MA. Magnetocaloric effect in $La_{1.25}Sr_{0.75}MnCoO_6$. *J Therm Anal Calorim* 2013, DOI: 10.1007/s10973-013-3362-2.

[8] Hamad MA. Simulation of magnetocaloric effect in $La_{0.7}Ca_{0.3}MnO_3$ ceramics fabricated by fast sintering process. *J Supercond Nov Magn* 2013, DOI: 10.1007/s10948-013-2260-y.

[9] Hamad MA. Magneto-caloric effect in $Ge_{0.95}Mn_{0.05}$ films. *J Supercond Nov Magn* 2013, **26**: 449–453.

[10] Hamad MA. Magnetocaloric effect in $La_{0.7}Sr_{0.3}MnO_3/Ta_2O_5$ composites. *J Adv Ceram* 2013, **2**: 213–217.

[11] Hamad MA. Theoretical work on magnetocaloric effect in ceramic and sol–gel $La_{0.67}Ca_{0.33}MnO_3$. *J Therm Anal Calorim* 2013, **111**: 1251–1254.

[12] Hamad MA. Magnetocaloric effect of perovskite manganites $Ce_{0.67}Sr_{0.33}MnO_3$. *J Supercond Nov Magn* 2013, DOI: 10.1007/s10948-013-2124-5.

[13] Hamad MA. Theoretical investigations on electrocaloric properties of $PbZr_{0.95}Ti_{0.05}O_3$ thin film. *Int J Thermophys* 2013, **34**: 1158–1165.

[14] Hamad MA. Magnetocaloric effect in nanopowders of $Pr_{0.67}Ca_{0.33}Fe_xMn_{1-x}O_3$. *J Supercond Nov Magn* 2013, DOI: 10.1007/s10948-013-2244-y.

[15] Hamad MA. Magnetocaloric effect of perovskite $Eu_{0.5}Sr_{0.5}CoO_3$. *J Supercond Nov Magn* 2013, DOI: 10.1007/s10948-013-2270-9.

[16] Hamad MA. Magnetocaloric effect in (001)-oriented MnAs thin film. *J Supercond Nov Magn* 2013, DOI: 10.1007/s10948-013-2254-9.

[17] Keogh D, Chen Z, Hughes RA, *et al*. (100) $MgAl_2O_4$ as a lattice-matched substrate for the epitaxial thin film deposition of the relaxor ferroelectric PMN–PT. *Appl Phys A* 2010, **98**: 187–194.

[18] Kamzina LS, Snetkova EV, Raevskiĭ IP, *et al*. Evolution of the ferroelectric phase in <001>-oriented $(100-x)PbMg_{1/3}Nb_{2/3}O_3$–$xPbTiO_3$ single crystals. *Phys Solid State*+ 2007, **49**: 762–768.

[19] Yang Y, Liu YL, Ma SY, *et al*. Polarized micro-Raman study of the field-induced phase transition in the relaxor $0.67PbMg_{1/3}Nb_{2/3}O_3$–$0.33PbTiO_3$ single crystal. *Appl Phys Lett* 2009, **95**: 051911.

[20] Correia TM, Young JS, Whatmore RW, *et al*. Investigation of the electrocaloric effect in a $PbMg_{2/3}Nb_{1/3}O_3$–$PbTiO_3$ relaxor thin film. *Appl Phys Lett* 2009, **95**: 182904.

[21] Zeng M, Or SW, Chan HLW. Effect of phase transformation on the converse magnetoelectric properties of a heterostructure of $Ni_{49.2}Mn_{29.6}Ga_{21.2}$ and $0.7PbMg_{1/3}Nb_{2/3}O_3$–$0.3PbTiO_3$ crystals. *Appl Phys Lett* 2010, **96**: 182503.

[22] Rodriguez BJ, Jesse S, Morozovska AN, *et al*. Real space mapping of polarization dynamics and hysteresis loop formation in relaxor-ferroelectric $PbMg_{1/3}Nb_{2/3}O_3$–$PbTiO_3$ solid solutions. *J Appl Phys* 2010, **108**: 042006.

[23] Hamad MA. Room temperature giant electrocaloric properties of relaxor ferroelectric 0.93PMN–0.07PT thin film. *AIP Advances* 2013, **3**: 032115.

[24] Hamad MA. Calculation of electrocaloric properties of ferroelectric $SrBi_2Ta_2O_9$. *Phase Transitions* 2012, **85**: 159–168.

[25] Hamad MA. Magnetocaloric effect in $La_{1-x}Cd_xMnO_3$. *J Supercond Nov Magn* 2013, DOI: 10.1007/s10948-013-2189-1.

[26] Wood ME, Potter WH. General analysis of magnetic refrigeration and its optimization using a new concept: Maximization of refrigerant capacity. *Cryogenics* 1985, **25**: 667–683.

[27] Dkhil B, Kiat JM. Electric-field-induced polarization in the ergodic and nonergodic states of $PbMg_{1/3}Nb_{2/3}O_3$ relaxor. *J Appl Phys* 2001, **90**: 4676.

[28] He Y, Li XM, Gao XD, *et al*. Enhanced electrocaloric properties of PMN–PT thin films with LSCO buffer layers. *Funct Mater Lett* 2011, **4**: 45.